BULLETIN OF THE POLISH ACADEMY OF SCIENCES
TECHNICAL SCIENCES, Vol. 71(4), 2023, Article number: e145567
DOI: 10.24425/bpasts.2023.145567

MECHANICAL AND AERONAUTICAL ENGINEERING, THERMODYNAMICS

Influence of material distribution and damping on the dynamic stability of Bernoulli-Euler beams

Sebastian GARUS[1]*, Justyna GARUS[1], Wojciech SOCHACKI[1], Marcin NABIAŁEK[2], Jana PETRŮ[3], Wojciech BOREK[4], Michal ŠOFER[5], and Paweł KWIATOŃ[1]

[1] Faculty of Mechanical Engineering and Computer Science, Czestochowa University of Technology, Poland
[2] Faculty of Production Engineering and Materials Technology, Department of Physics, Czestochowa University of Technology, Armii Krajowej 19, 42-201 Czestochowa, Poland
[3] Department of Machining, Assembly and Engineering Metrology, Faculty of Mechanical Engineering, VSB-Technical University of Ostrava, 70833 Ostrava, Czech Republic
[4] Department of Engineering Materials and Biomaterials, Silesian University of Technology, Konarskiego 18A, 44-100 Gliwice, Poland
[5] Department of Applied Mechanics, Faculty of Mechanical Engineering, VSB—Technical University of Ostrava, 17. listopadu 2172/15, 70800 Ostrava, Czech Republic

Abstract. The study analyzed the influence of materials and different types of damping on the dynamic stability of the Bernoulli-Euler beam. Using the mode summation method and applying an orthogonal condition of eigenfunctions and describing the analyzed system with the Mathieu equation, the problem of dynamic stability was solved. By examining the influence of internal and external damping and damping in the beam supports, their influence on the regions of stability and instability of the solution to the Mathieu equation was determined.

Key words: mechanical vibrations; damping; beam; dynamic stability; Mathieu equation.

1. INTRODUCTION

At the beginning of the second half of the 19th century, during the construction of railway bridges, it was already noticed that the damage to the structure resulted from the loss of stability of thin plates, shells, and slender bars. Examples of such damage can be seen in the works [1, 2], and one of the most famous was the Tacoma Narrows Bridge (TNB) from 1940 due to the film showing the oscillation and destruction of the bridge [3]. These types of events initiated intensive research in the field of dynamic stability.

Already in 1744, Leonard Euler described the basics of structural stability in his work [4]. He solved the problem of axial compression of an ideal bar with different support methods. In 1773, Lagrange worked on the optimization of the shape of a column loaded with an axial force [5, 6]. The problem is important because the search for the most optimal geometries for given applications is still ongoing [7–9]. The first work on a non-conservative loading force was Beck's work from 1952 [10], in which the influence of loading the tracking force on the end of the column on its stability was analyzed.

There are various theories describing the kinematics of column deformation, understood as a slender and simple structural element subjected to compression. They are described in more detail in [11], and the most important of them are the theories of Bernoulli-Euler [12], Timoshenko [13], or Reddy-Bickford [14, 15]. The last of them was further developed in [16]. The subject of buckling of columns and structures was described in the literature, inter alia, in [17], and dynamic stability in [18]. The comparison of selected theories was presented in [19]. In this work, the columns according to the Bernoulli-Euler theory will be analyzed.

Using the dynamic stability criterion and determining the eigenvalues defining the correlations of the eigenfrequencies of the tested mechanical system to the load parameter, resulting from the solution of the differential equation of motion taking into account the boundary conditions, it allows the stability of a given system to be tested and its type to be determined. Leipholtz in [20] showed divergent and flutter types of stability, while Sundararajan in [21] also showed hybrid systems combining features of both types. The stability of the columns is also influenced by other specific factors, for example, Kordas and Życzkowski in [22] analyzed the influence of the tracking coefficient on the critical force for the cantilever column, while the natural frequency and stability for the Beck column were investigated by Sundararajan in [23] when the end of the column was resiliently supported. The passage through the stability limit is described in [24]. Kounadis investigated the influence of the stiffness coefficient of the springs used to support the bar on the loss of stability [25]. In the work [26], the influ-

*e-mail: sebastian.garus@pcz.pl

Manuscript submitted 2023-02-08, revised 2023-03-04, initially accepted for publication 2023-03-10, published in August 2023.

ence of the inertia of rotation and the shear force in the Beck commune with the flutter-type force was also considered. The instability of the column was also analyzed in [27].

A special case of parametric vibrations, in which structures are loaded with a periodic function of time, is called dynamic stability [28]. Parametric resonances in the dynamic stability analysis play a fundamental role. In the region of unstable solutions, the amplitude of resonant vibrations increases unlimitedly. Most of the work on dynamic stability focuses on simple beam systems with interconnected discrete elements [29–33], as many mechanical systems can be modeled with them.

During the operation of various types of machines, mechanical vibrations very often occur as an undesirable element. This phenomenon adversely affects the strength of the working elements and may cause their faster wear, but more importantly, they cause health problems for people operating these machines, such as disorders in the vascular, nervous, and osteoarticular systems, and may also cause problems with visual acuity or problems with motor coordination. The influence of noise is also important. The above harmful phenomena caused by vibrations have been described in [34, 35]. To minimize the negative effects of vibrations as much as possible, the damping phenomenon is used, in which the dissipation of mechanical energy occurs due to the occurrence of frictional forces during vibrations. The phenomenon of damping and its influence on mechanical systems exposed to vibrations has been described in the works of Osiński [36] and Giergiel [37]. If the natural methods of damping (internal friction in the material, environmental impact, friction in joints and supports) are not sufficient, additional special vibration dampers are used, such as dynamic and active vibration eliminators [38]. Moreover, vibration isolation is also used, placed between the insulated system and the vibrating system, made of additional structural elements or their assemblies [39]. Damping is a phenomenon that always occurs during mechanical vibrations [34, 39, 40].

Even small vibrations in the machine can cause the phenomenon of resonance [41] and lead to its destruction. The use of damping will reduce the risk of this phenomenon. Damping, depending on its mechanism and source, can be divided into internal damping in a viscoelastic material [42, 43], design damping in movable connections [44, 45], design damping in fixed connections (so-called dry friction) [46, 47], viscous resistance (e.g. the external influence of the medium) [48, 49].

This study investigated how different types of damping affect the dynamic stability of Bernoulli-Euler beams. Using the perturbation method, the stability regions of the solution of the equation of motion transformed into the form of the Mathieu equation were determined.

2. MATHEMATICAL MODEL

Figure 1 shows a Bernoulli-Euler beam, articulated at its ends, loaded with an axial compressive force described by the relation $P(t) = P_0 + S\cos \nu t$, where P_0 is the constant component of the longitudinal force, S is the variable component of the longitudinal force, $W(x,t)$ is the transverse displacement of the beam at location x and time t, ν is the frequency of the exciting force,

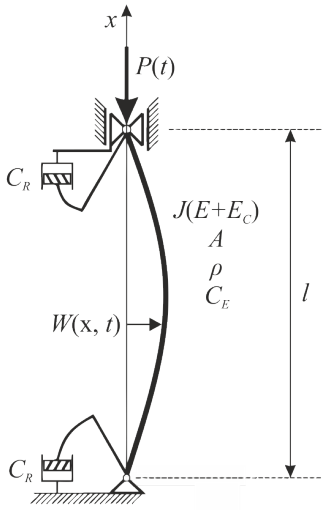

Fig. 1. A simple Bernoulli-Euler beam loaded with an axial compressive force that changes cyclically, taking into account different types of damping

and t is time. The material properties of the beam are Young's modulus E, the moment of inertia J of the cross-section, the cross-sectional area A, and the material density ρ. The added damping is due to the resistance to movement in the supports – they are modeled with C_R rotary dampers and the damping is caused by the external viscous resistance C_E. The viscosity index of the material was denoted by E_C.

The problem of transverse vibrations of a straight Bernoulli-Euler beam was solved by formulating the boundary problem using Hamilton's variational principle

$$\int_{t_1}^{t_2} (\delta T - \delta V)\,\mathrm{d}t + \int_{t_1}^{t_2} (-\delta W_N)\,\mathrm{d}t = 0. \tag{1}$$

Equation (1) takes into account the variation of the virtual work of non-conservative forces as

$$\begin{aligned}\delta W_N = {} & E_C J \frac{\partial^3 W(l,t)}{\partial x^2 \partial t}\delta\frac{\partial W(l,t)}{\partial x} - E_C J \frac{\partial^3 W(0,t)}{\partial x^2 \partial t}\delta\frac{\partial W(0,t)}{\partial x} \\ & - E_C J \frac{\partial^4 W(l,t)}{\partial x^3 \partial t}\delta W(l,t) + E_C J \frac{\partial^4 W(0,t)}{\partial x^3 \partial t}\delta W(0,t) \\ & + \int_0^l E_C J \frac{\partial^5 W(x,t)}{\partial x^4 \partial t}\delta W(x,t)\,\mathrm{d}x + \int_0^l C_E \frac{\partial W(x,t)}{\partial t}\delta W(x,t)\,\mathrm{d}x \\ & + C_R \frac{\partial^2 W(0,t)}{\partial x \partial t}\delta\frac{\partial W(0,t)}{\partial x} - C_R \frac{\partial^2 W(l,t)}{\partial x \partial t}\delta\frac{\partial W(l,t)}{\partial x}. \end{aligned} \tag{2}$$

The variation of the bending spring energy is

$$\begin{aligned}\delta V_1 = {} & EJ \frac{\partial^2 W(l,t)}{\partial x^2}\delta\frac{\partial W(l,t)}{\partial x} - EJ \frac{\partial^2 W(0,t)}{\partial x^2}\delta\frac{\partial W(0,t)}{\partial x} \\ & - EJ \frac{\partial^3 W(l,t)}{\partial x^3}\delta W(l,t) + EJ \frac{\partial^3 W(0,t)}{\partial x^3}\delta W(0,t) \\ & + \int_0^l EJ \frac{\partial^4 W(x,t)}{\partial x^4}\delta W(x,t)\,\mathrm{d}x. \end{aligned} \tag{3}$$

On the other hand, the variation in energy from the external load is

$$\delta V_2 = \int_0^l P(t)\frac{\partial^2 W(x,t)}{\partial x^2}\delta W(x,t)\,\mathrm{d}x - P(t)\frac{\partial W(l,t)}{\partial x}\delta W(l,t) + P(t)\frac{\partial W(0,t)}{\partial x}\delta W(0,t). \tag{4}$$

The variation in kinetic energy is defined as

$$\delta T = -\int_0^l \rho A\frac{\partial^2 W(x,t)}{\partial t^2}\delta W(x,t)\,\mathrm{d}x. \tag{5}$$

Substituting equation (2)–(5) to equation (1), the differential equation of the motion of the beam transverse vibrations was determined as

$$\frac{\partial^4 W(x,t)}{\partial x^4} + \frac{E_C}{E}\frac{\partial^5 W(x,t)}{\partial x^4 \partial t} + \frac{\rho A}{JE}\frac{\partial^2 W(x,t)}{\partial t^2} + \frac{P(t)}{JE}\frac{\partial^2 W(x,t)}{\partial x^2} + \frac{C_E}{JE}\frac{\partial W(x,t)}{\partial t} = 0. \tag{6}$$

The solution of equation (6) is predicted as a series of eigenfunctions

$$W(x,t) = \sum_{n=1}^{\infty} W_n(x)T_n(t), \tag{7}$$

where $W_n(x)$ is the nth natural modes of vibrations and $T_n(t)$ is an unknown time function.

The first form of vibration is of major importance, so the displacement $W(x,t)$ is written in the form of the product of functions with variables separated by time t and the coordinate x

$$W(x,t) = W(x)T(t) = W(x)e^{i\omega t}. \tag{8}$$

After separating the space and time variables and substituting $d^2 = P/(JE + i\omega JE_C)$, $\Omega^2 = \left(\rho A\omega^2 - i\omega C_E\right)/(JE + i\omega JE_C)$, the equation of motion takes the form

$$\frac{d^4 W(x)}{dx^4} + d^2\frac{d^2 W(x)}{dx^2} - \Omega^2 W(x) = 0. \tag{9}$$

For the system shown in Fig. 1, the boundary conditions after separating the variables are as follows

$$W(0) = W(l) = 0, \tag{10}$$

$$J(E + i\omega E_C)\frac{d^2 W(0)}{dx^2} = i\omega C_R\frac{dW(0)}{dx}, \tag{11}$$

$$J(E + i\omega E_C)\frac{d^2 W(l)}{dx^2} = -i\omega C_R\frac{dW(l)}{dx}. \tag{12}$$

The general solution to the displacement equation (9) is a function

$$W(x) = C_1\cosh(\alpha x) + C_2\sinh(\alpha x) + C_3\cos(\beta x) + C_4\sin(\beta x), \tag{13}$$

where

$$\alpha = \sqrt{-\frac{1}{2}d^2 + \sqrt{\frac{1}{4}d^4 + \Omega^2}}, \tag{14}$$

$$\beta = \sqrt{\frac{1}{2}d^2 + \sqrt{\frac{1}{4}d^4 + \Omega^2}}. \tag{15}$$

Substituting solution equation (13) into equations (10)–(12), a homogeneous system of equations A was obtained with respect to unknown constants C_i. This matrix system is written as

$$[A](\omega)C = 0, \tag{16}$$

where $[A](\omega) = [a_{pq}]$; $[p,q] = (1-4)$, and $C = [C_i]^T$; $i = 1-4$.

In the case when the determinant of the matrix of coefficients is equal to zero for the constants C_i, the system has a non-trivial solution

$$\det A(\omega) = 0. \tag{17}$$

Equation (17) allows to determine the dependence of the eigenfrequencies of the system ω_i on the load P and to determine the value of the critical load P_k.

To expand the eigenfunctions into a series equation (7), their orthogonality was assumed. Equation (9), after separating the variables for the n-th and m-th eigenfunctions and taking into account the boundary conditions, takes the form

$$\left(\frac{\rho A{\omega_n}^2 - i\omega_n C_E}{J(E + i\omega_n E_C)} - \frac{\rho A{\omega_m}^2 - i\omega_m C_E}{J(E + i\omega_m E_C)}\right) \times \int_0^l W_n(x)W_m(x)\,\mathrm{d}x = 0. \tag{18}$$

Since $\omega_m \neq \omega_n$, when $m \neq n$, then the orthogonality condition sought is determined by the formula

$$\int_0^l W_n(x)W_m(x)\,\mathrm{d}x = \begin{cases} 0 & m \neq n, \\ \gamma_m^2 = \int_0^l W_m^2(x)\,\mathrm{d}x & m = n. \end{cases} \tag{19}$$

Equation (6) was substituted with equation (7) and obtained

$$\sum_{n=1}^{\infty}\left(JE\frac{d^4 W_n(x)}{dx^4}T_n(t) + JE_C\frac{d^4 W_n(x)}{dx^4}\frac{dT_n(t)}{dt} + P_0\frac{d^2 W_n(x)}{dx^2}T_n(t) + S\cos(\nu t)\frac{d^2 W_n(x)}{dx^2}T_n(t) + W_n(x)\rho A\frac{d^2 T_n(t)}{dt^2} + W_n(x)C_E\frac{dT_n(t)}{dt}\right) = 0. \tag{20}$$

Equation (20) multiplied by m-th eigenfunction $W_m(x)$ takes the form

$$\sum_{n=1}^{\infty}\left(\left(JE\frac{d^4W_n(x)}{dx^4}W_m(x)+P_0\frac{d^2W_n(x)}{dx^2}W_m(x)\right)T_n(t)\right.$$
$$+\,JE_C\frac{d^4W_n(x)}{dx^4}W_m(x)\frac{dT_n(t)}{dt}$$
$$+\,S\cos(\nu t)\frac{d^2W_n(x)}{dx^2}W_m(x)T_n(t)+W_n(x)W_m(x)\rho A\frac{d^2T_n(t)}{dt^2}$$
$$\left.+\,W_n(x)W_m(x)C_E\frac{dT_n(t)}{dt}\right)=0. \tag{21}$$

Multiplied by the functions $W_m(x)$ equation (9) after separating the variables for the n-th eigenfunction and minor transformations takes the form

$$JE\frac{d^4W_n(x)}{dx^4}W_m(x)+P_0\frac{d^2W_n(x)}{dx^2}W_m(x)$$
$$=\left(\rho A\omega^2-i\omega C_E\right)W_n(x)W_m(x)$$
$$-\,i\omega JE_C\frac{d^4W_n(x)}{dx^4}W_m(x). \tag{22}$$

Substituting equation (22) into equation (21) gives

$$\sum_{n=1}^{\infty}\left[\left(\left(\rho A\omega^2-i\omega C_E\right)W_n(x)W_m(x)\right.\right.$$
$$-\,i\omega JE_C\frac{d^4W_n(x)}{dx^4}W_m(x)+S\cos(\nu t)\frac{d^2W_n(x)}{dx^2}W_m(x)\Big)T_n(t)$$
$$+\left(JE_C\frac{d^4W_n(x)}{dx^4}W_m(x)+W_n(x)W_m(x)C_E\right)\frac{dT_n(t)}{dt}$$
$$\left.+\,\rho AW_n(x)W_m(x)\frac{d^2T_n(t)}{dt^2}\right]=0. \tag{23}$$

Only the first term of the sum in equation (7) is of significant importance, as shown in [50]. The work analyzes the parametric resonance for the first (fundamental) vibration frequency of the system $n=1$, which, taking into account the orthogonality condition (18), allows to transform equation (23) into the form

$$T(t)\left[\left(\rho A\omega^2-i\omega C_E\right)\int_0^l W^2(x)\,\mathrm{d}x\right.$$
$$\left.-\,i\omega JE_C\int_0^l\frac{d^4W(x)}{dx^4}W(x)\,\mathrm{d}x+S\cos(\nu t)\int_0^l\frac{d^2W(x)}{dx^2}W(x)\,\mathrm{d}x\right]$$
$$+\,\frac{d^2T(t)}{dt^2}\rho A\int_0^l W^2(x)\,\mathrm{d}x$$
$$+\,\frac{dT(t)}{dt}\left(JE_C\int_0^l\frac{d^4W(x)}{dx^4}W(x)dx\right.$$
$$\left.+C_E\int_0^l W^2(x)\,\mathrm{d}x\right)=0. \tag{24}$$

Dividing both sides of equation (24) by $-\rho A\int_0^l W^2(x)\,\mathrm{d}x$ and substituting $\tau=\nu t$ we get

$$\frac{d^2T(\tau)}{d\tau^2}+\left(\frac{C_E}{\rho A\nu^2}+\frac{JE_C\int_0^l\frac{d^4W(x)}{dx^4}W(x)\,\mathrm{d}x}{\rho A\nu^2\int_0^l W^2(x)\,\mathrm{d}x}\right)\frac{dT(\tau)}{d\tau}$$
$$+\left(\frac{\omega^2}{\nu^2}-\frac{i\omega C_E}{\rho A\nu^2}-\frac{i\omega JE_C\int_0^l\frac{d^4W(x)}{dx^4}W(x)\,\mathrm{d}x}{\rho A\nu^2\int_0^l W^2(x)\,\mathrm{d}x}\right.$$
$$\left.+\frac{\int_0^l\frac{d^2W(x)}{dx^2}W(x)\,\mathrm{d}x}{\rho A\nu^2\int_0^l W^2(x)\,\mathrm{d}x}S\cos(\nu\tau)\right)T(\tau)=0. \tag{25}$$

The equation of motion (25) has the form of the damped Mathieu equation presented in [51] as

$$\frac{d^2T(\tau)}{d\tau^2}+c\frac{dT(\tau)}{d\tau}+(\delta+\varepsilon\cos\tau)\,T(\tau)=0, \tag{26}$$

where

$$c=\frac{C_E+b}{\rho A\nu^2}, \tag{27}$$

$$\delta=\frac{\omega^2}{\nu^2}-\frac{i\omega(C_E+b)}{\rho A\nu^2}, \tag{28}$$

$$\varepsilon=\frac{S\int_0^l\frac{d^2W(x)}{dx^2}W(x)\,\mathrm{d}x}{\rho A\nu^2\int_0^l W^2(x)\,\mathrm{d}x} \tag{29}$$

and

$$b=\frac{JE_C\int_0^l\frac{d^4W(x)}{dx^4}W(x)\,\mathrm{d}x}{\int_0^l W^2(x)\,\mathrm{d}x}. \tag{30}$$

In order to determine the influence of damping on the transition curves in the Mathieu equation (26), the two-variable expansion method was used [52–55]. To apply the perturbation method, the damping coefficient c was scaled to $O(\varepsilon)$ by $c=\varepsilon\mu$, which, assuming small values of ε and substituting

$\xi = \tau$ and $\eta = \varepsilon\tau$ to equation (26) and performing appropriate transformations, leads to

$$\frac{\partial^2 T(\xi,\eta)}{\partial\xi^2} + 2\varepsilon\frac{\partial^2 T(\xi,\eta)}{\partial\xi\partial\eta} + \varepsilon^2\frac{\partial^2 T(\xi,\eta)}{\partial\eta^2} + \varepsilon\mu\left(\frac{\partial T(\xi,\eta)}{\partial\xi} + \varepsilon\frac{\partial T(\xi,\eta)}{\partial\eta}\right) + (\delta + \varepsilon\cos\xi)\,T(\xi,\eta) = 0. \tag{31}$$

By expanding the function $T(\xi,\eta)$ and δ into power series and omitting the factor $O(\varepsilon^2)$ and then prioritizing by ε successive powers, the following system of equation was obtained

$$\frac{\partial^2 T_0(\xi,\eta)}{\partial\xi^2} + \delta T_0(\xi,\eta) = 0, \tag{32}$$

$$\frac{\partial^2 T_1(\xi,\eta)}{\partial\xi^2} + \delta T_1(\xi,\eta) = -2\frac{\partial^2 T_0(\xi,\eta)}{\partial\xi\partial\eta} - \mu\frac{\partial T_0(\xi,\eta)}{\partial\xi} - T_0(\xi,\eta)\cos\xi, \tag{33}$$

$$2\frac{\partial^2 T_1(\xi,\eta)}{\partial\xi\partial\eta} + \mu\frac{\partial T_1(\xi,\eta)}{\partial\xi} + T_1(\xi,\eta)\cos\xi = -\frac{\partial^2 T_0(\xi,\eta)}{\partial\eta^2} - \mu\frac{\partial T_0(\xi,\eta)}{\partial\eta}, \tag{34}$$

$$\frac{\partial^2 T_1(\xi,\eta)}{\partial\eta^2} + \mu\frac{\partial T_1(\xi,\eta)}{\partial\eta} = 0. \tag{35}$$

Equation (32) is an equation of motion of a simple harmonic oscillator and its general solution takes the form

$$T_0(\xi,\eta) = A(\eta)\cos\sqrt{\delta}\xi + B(\eta)\sin\sqrt{\delta}\xi. \tag{36}$$

It is worth noting that the amplitudes of the general solution depend on η. Substituting equation (36) into equation (33) transforming and converting the products of trigonometric functions into sums, we obtained

$$\begin{aligned}\frac{\partial^2 T_1(\xi,\eta)}{\partial\xi^2} + \delta T_1(\xi,\eta) &= 2\frac{\mathrm{d}A(\eta)}{\mathrm{d}\eta}\sqrt{\delta}\sin\sqrt{\delta}\xi - 2\frac{\mathrm{d}B(\eta)}{\mathrm{d}\eta}\sqrt{\delta}\cos\sqrt{\delta}\xi \\ &+ \mu A(\eta)\sqrt{\delta}\sin\sqrt{\delta}\xi - \mu B(\eta)\sqrt{\delta}\cos\sqrt{\delta}\xi \\ &- \frac{A(\eta)}{2}\left(\cos\left(\sqrt{\delta}+1\right)\xi + \cos\left(\sqrt{\delta}-1\right)\xi\right) \\ &- \frac{B(\eta)}{2}\left(\sin\left(\sqrt{\delta}+1\right)\xi - \sin\left(\sqrt{\delta}-1\right)\xi\right).\end{aligned} \tag{37}$$

The first two terms on the right side of the equation represent resonance conditions and may cause the solution to become unstable. If $\mathrm{d}A(\eta)/\mathrm{d}\eta = 0$ and $\mathrm{d}B(\eta)/\mathrm{d}\eta = 0$ the $\cos t$ term of Mathieu's equation does not affect the solution and there is no parametric resonance phenomenon. In the case of substituting $\delta = 1/4$ and $\mu = 0$ (no damping) to equation (37) and after transformations, the following is obtained

$$\begin{aligned}\frac{\partial^2 T_1(\xi,\eta)}{\partial\xi^2} + \frac{1}{4}T_1(\xi,\eta) &= \left(\frac{\mathrm{d}A(\eta)}{\mathrm{d}\eta} + \frac{B(\eta)}{2}\right)\sin\frac{\xi}{2} - \left(\frac{\mathrm{d}B(\eta)}{\mathrm{d}\eta} + \frac{A(\eta)}{2}\right)\cos\frac{\xi}{2} \\ &- \frac{A(\eta)}{2}\cos\frac{3\xi}{2} - \frac{B(\eta)}{2}\sin\frac{3\xi}{2},\end{aligned} \tag{38}$$

which allowed to obtain additional resonance conditions defined as $\mathrm{d}A(\eta)/\mathrm{d}\eta = -B(\eta)/2$, $\mathrm{d}B(\eta)/\mathrm{d}\eta = -A(\eta)/2$ which leads to $d^2A(\eta)/d\eta^2 = A(\eta)/4$. The value of the parameter $\delta = 1/4$ causes instability, and $A(\eta)$ and $B(\eta)$ increase exponentially. In the presented example, there is a subharmonic resonance in which the excitation frequency is twice the natural frequency.

After inserting the expansion into the power series δ with respect to ε to equation (33) and for $\mu = 0$ (no damping), the following was obtained

$$\frac{\partial^2 T_1(\xi,\eta)}{\partial\xi^2} + \frac{1}{4}T_1(\xi,\eta) = -2\frac{\partial^2 T_0(\xi,\eta)}{\partial\xi\partial\eta} - \delta_1 T_0(\xi,\eta) - T_0(\xi,\eta)\cos\xi \tag{39}$$

and the resonant conditions take the form of $\mathrm{d}A(\eta)/\mathrm{d}\eta = (\delta_1 - 1/2)B(\eta)$ and $\mathrm{d}B(\eta)/\mathrm{d}\eta = -(\delta_1 + 1/2)A(\eta)$ which leads to $d^2A(\eta)/d\eta^2 + (\delta_1 + 1/4)A(\eta) = 0$. The conditions fulfill the sine and cosine functions for $A(\eta)$ and $B(\eta)$, respectively, with $\delta_1^2 - 1/4 > 0$, i.e. when $\delta_1 > 1/2$ or $\delta_1 < -1/2$. The curves presented represent the stability curves in the space δ–ε as

$$\delta = \frac{1}{4} \pm \frac{\varepsilon}{2} + O(\varepsilon^2). \tag{40}$$

Equations (36) and (40) correspond to the region of instability with the zero point at $\delta = 1/4$. In the case of the damped system $\mu \neq 0$, equation (39) takes the form

$$\frac{\partial^2 T_1(\xi,\eta)}{\partial\xi^2} + \frac{1}{4}T_1(\xi,\eta) = -2\frac{\partial^2 T_0(\xi,\eta)}{\partial\xi\partial\eta} - \mu\frac{\partial T_0(\xi,\eta)}{\partial\xi} - \delta_1 T_0(\xi,\eta) - T_0(\xi,\eta)\cos\xi. \tag{41}$$

Suitable derivatives take the form of

$$\begin{cases}\dfrac{\mathrm{d}A(\eta)}{\mathrm{d}\eta} = -\dfrac{\mu}{2}A(\eta) + \left(\delta_1 - \dfrac{1}{2}\right)B(\eta), \\ \dfrac{\mathrm{d}B(\eta)}{\mathrm{d}\eta} = -\left(\delta_1 + \dfrac{1}{2}\right)A(\eta) - \dfrac{\mu}{2}B(\eta).\end{cases} \tag{42}$$

The above system of equations can be solved assuming solutions $A(\eta) = A_0 e^{\lambda\eta}$ and $B(\eta) = B_0 e^{\lambda\eta}$. A non-trivial solution is obtained for

$$\begin{vmatrix} -\dfrac{\mu}{2} - \lambda & -\dfrac{1}{2} + \delta_1 \\ -\dfrac{1}{2} + \delta_1 & -\dfrac{\mu}{2} - \lambda \end{vmatrix} = 0, \tag{43}$$

from which it follows that

$$\lambda = -\frac{\mu}{2} \pm \sqrt{-\delta_1^2 + \frac{1}{4}}. \tag{44}$$

To determine the transition between the stable and unstable state, $\lambda = 0$ should be assumed and the value of δ_1 should be determined as $\delta_1 = \pm\sqrt{1-\mu^2}/2$. For the first region of instability, a relationship was established

$$\begin{aligned}\delta &= \frac{1}{4} \pm \varepsilon \frac{\sqrt{1-\mu^2}}{2} + O\left(\varepsilon^2\right) \\ &= \frac{1}{4} \pm \frac{\sqrt{\varepsilon^2 - c^2}}{2} + O\left(\varepsilon^2\right).\end{aligned} \tag{45}$$

Using the relation (45), the influence of the damping constant c on the first unstable region of the Mathieu equation is shown in Fig. 2. With the increase of the damping coefficient, the region of unstable solutions of the equation decreased. The minimum value of the coefficient ε increased its value with the increase of the damping constant c and a larger and larger region of possible stable solutions arose under the transition curve dividing the static and unstable regions.

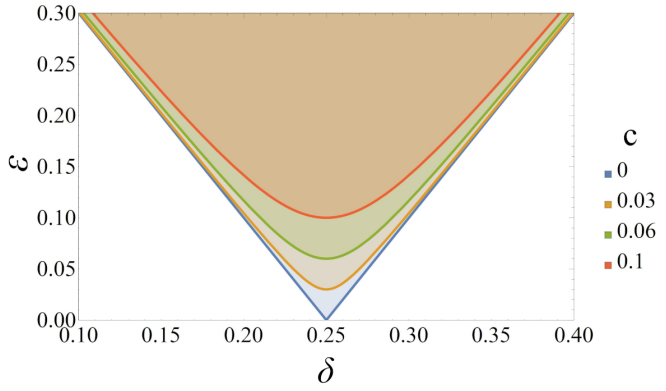

Fig. 2. Influence of viscous damping c on the unstable (shaded) region of the solution to the Mathieu equation

3. NUMERICAL RESULTS

The paper solves the problem of dynamic stability of an undamped straight Bernoulli-Euler beam, articulated at its ends and loaded with cyclically changing axial compressive force. The Wolfram Mathematica package was used, for which proprietary software was prepared to perform calculations and make drawings. The beam length was assumed to be $l = 3$ m and a square cross-section with a side $h = 0.3$ m and a surface area $A = 0.09$ m^2. The value of the critical axial compressive force for steel was assumed to be $P_k = 9.32676 \times 10^7$ N, the constant load component was $P_0 = 5\%P_k$, similarly, the variable load component was $S = 5\%P_k$. The area of inertia of the cross-section was determined from the relationship $J = h^4/12 = 675 \times 10^{-6}$ m^4. The material properties of the beams for the various materials used in the simulation are summarized in Table 1. The first three eigenfrequencies of the analyzed beams were determined and collected in Table 2.

Table 1
Properties of materials used for the analysis of dynamic stability of Bernoulli-Euler beams [56]

Material	E [GPa]	ρ [kg/m^3]
Steel	210	7860
Copper	125	8900
Aluminum	70	2700
Titanium	116	4500

Table 2
Determined eigenfrequencies of beams

Material	ω_1 [rad/s]	ω_2 [rad/s]	ω_3 [rad/s]
Steel	483.473	1956.19	4410.66
Copper	346.831	1414.67	3194.26
Aluminum	461.292	1912.38	4330.27
Titanium	468.905	1915.59	4326.52

Based on the determined shapes of the displacement functions for the given materials, the parameters δ and ε of the Mathieu equation from equations (28) and (29) were determined and plotted on the Strutt chart in Fig. 3. The frequencies of the exciting force were determined for a given first natural frequency for a given material according to the dependence $\nu_n = 2\omega_1/n$, where $n \in \{1,2,3,4\}$.

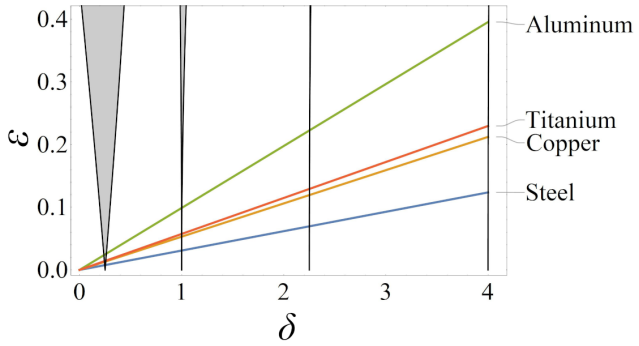

Fig. 3. Relations between the coefficients ε and δ for the analyzed materials plotted on the Strutt chart

As can be seen in Fig. 3, the beam made of aluminum was characterized by the lowest dynamic stability with the same geometric dimensions and load. Beams made of titanium and copper, despite large differences in natural frequencies, were characterized by similar dynamic stability in favor of the column made of copper. On the other hand, the most favorable results were obtained for the column made of steel.

In order to analyze the influence of various types of damping on the dynamic stability of the analyzed beam, dimensionless damping coefficients were introduced for the internal damping C_h, the external damping C_n and the structural damping in the

beam supports C_m in the form

$$C_h = \frac{E_C}{E\sqrt{l^4 \frac{\rho A}{EJ}}}, \tag{46}$$

$$C_n = \frac{C_E l^2}{\sqrt{\rho AEJ}}, \tag{47}$$

$$C_m = \frac{C_R}{l\sqrt{\rho AEJ}}. \tag{48}$$

The paper analyzes the influence of various types of damping on the dynamic stability of a steel beam with a geometry corresponding to the case under consideration without damping. The damping parameters for the considered cases are summarized in Table 3, the determined values of the eigenfrequencies ω_i, the damping coefficient c influencing the shape of the transition curve between the stable and unstable regions of the solution to the Mathieu equation and the determined coefficient ε for the first unstable region of the ε–δ system are also presented there.

The relations between the coefficients of the Mathieu equation plotted on the Strutt chart in the ε–δ system for the analyzed cases are presented in Fig. 4–8. The system without damping is shown in Fig. 4. An area was observed for which the solution to the Mathieu equation has unstable solutions (shaded area). The addition of damping in the beam supports increased the stability of the system (Fig. 5) but did not eliminate the unstable area. Properly selected medium damping reduced the unstable area (Fig. 6) and made the system in the entire an-

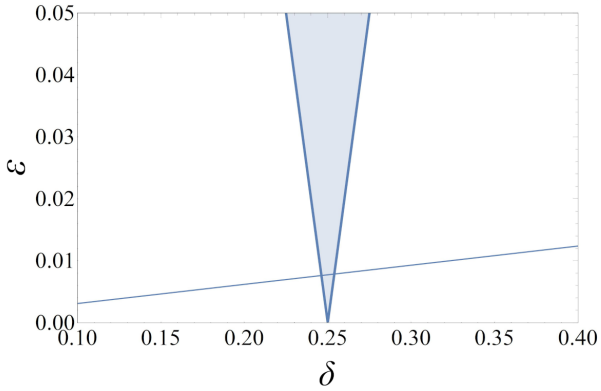

Fig. 4. Relations between the coefficients ε and δ for the analyzed materials plotted on the Strutt chart; no damping (case 1 in Table 3)

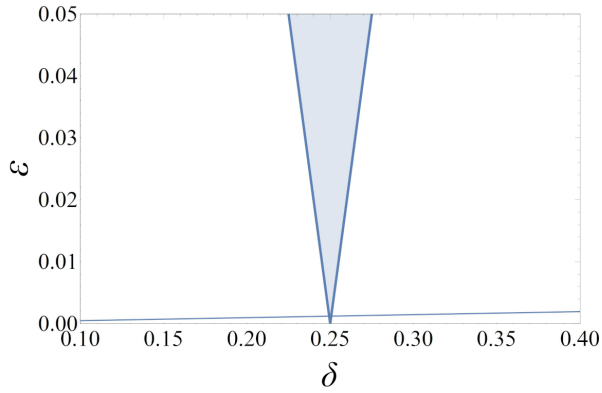

Fig. 5. Relations between the coefficients ε and δ for the analyzed materials plotted on the Strutt chart; considered damping in the beam supports for $C_m = 0.05$ (case 2 in Table 3)

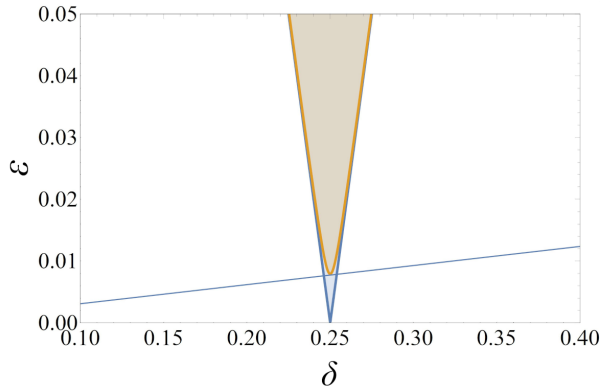

Fig. 6. Relations between the coefficients ε and δ for the analyzed materials plotted on the Strutt chart; medium damping for $C_n = 18.5$ is taken into account (case 3 in Table 3)

Table 3
Determined eigenfrequencies of beams made of structural steel for selected damping cases

Case	1	2	3	4	5
C_h	0	0	0	0.001	0
C_n	0	0	18.5	0	4.26
C_m	0	0.05	0	0	0.017
ω_1	483.473	$483.26 + 49.454i$	$150.569 + 459.429i$	$483.467 + 2.42246i$	$467.957 + 122.511i$
ω_2	1956.19	$1973.03 + 198.266i$	$1901.48 + 459.429i$	$1955.81 + 38.7593i$	$1951.55 + 171.862i$
ω_3	4410.66	$4486.25 + 443.051i$	$4386.67 + 459.429i$	$4406.29 + 196.219i$	$4413.77 + 253.874i$
c	0	0	$0.00792 + 0.00582i$	$5.181 \times 10^{-6} - 5.193 \times 10^{-8} i$	$0.00889 - 0.00011I$
σ	0.25	0.25	$0.20151 - 0.14797i$	$0.24999 - 0.00251i$	$0.22224 - 0.10602i$
ε	0.00773	$0.00121 + 0.01004i$	$0.00623 - 0.00458i$	$0.00773 - 0.00008i$	$0.00762 - 0.00036i$

alyzed range of δ had stable solutions. The internal damping did not cause any significant changes in the stability in relation to the undamped system (Fig. 7). The use of a combination of the damping of the center and supports (Fig. 8) significantly influenced the achievement of dynamic stability in the analyzed area of solutions, as well as allowed to reduce of the damping coefficient of supports.

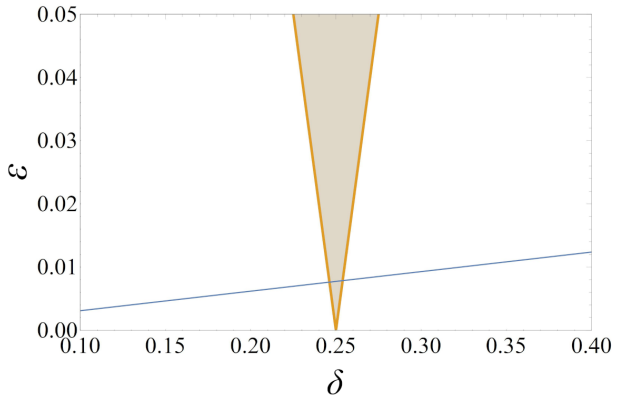

Fig. 7. Relations between the coefficients ε and δ for the analyzed materials plotted on the Strutt chart; internal damping taken into account for $C_h = 0.001$ (case 4 in Table 3)

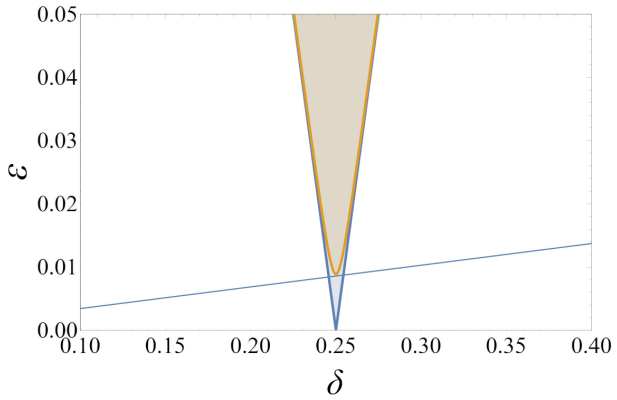

Fig. 8. Relations between the coefficients ε and δ for the analyzed materials plotted on the Strutt chart; considered damping of the medium for $C_n = 4.26$ and damping in the beam supports for $C_m = 0.017$ (case 5 in Table 3)

4. CONCULSIONS

The study investigated the influence of various materials on the dynamic stability of the Bernoulli-Euler beam, which showed that the dynamic stability of such beams increases with the increase of their Young's modulus (solutions for specific material data on longer sections lie in the stable areas).

The influence of different types of damping on the dynamic stability of a steel homogeneous Bernoulli-Euler beam, articulated with rotational dampers at its ends and loaded with an axial force (varying in time), was also investigated. The conducted tests showed that the internal damping does not significantly change the dynamic stability of the analyzed system. The use of damping in beam supports increases the stability of the system. The damping of the medium surrounding the beam has the most significant influence on the dynamic stability of the system under consideration. This type of damping narrows the areas of unstable solutions and causes the system to have stable solutions in the entire analyzed range.

The use of a viscous damper system suitably attached at different points on the beam could simulate a change in medium damping and eliminate unstable areas.

ACKNOWLEDGEMENTS

This publication was financed by the Ministry of Education and Science of Poland as the statutory financial grant of the Department of Mechanics and Machine Design Fundamentals of Czestochowa University of Technology.

The project is co-financed by the Governments of Czechia, Hungary, Poland and Slovakia through Visegrad Grants from International Visegrad Fund. The mission of the fund is to advance ideas for sustainable regional cooperation in Central Europe.

REFERENCES

[1] B. Akesson, *Understanding Bridges Collapses*. London: CRC Press, Taylor & Francis Group, 2008.

[2] D. Imhof, "Risk assessment of existing bridge structure," Ph.D. dissertation, University of Cambridge, 2004.

[3] "Tacoma narrows bridge collapse," http://www.youtube.com/watch?v=3mclp9QmCGs, 1940.

[4] L. Euler, *A method for finding curved lines enjoying properties of maximum or minimum, or solution of isoperimetric problems in the broadest accepted sense* (in Latin). Lausanæ et Genevæ: M.M. Bousquet et Soc. In (Euler, OO, Series I, 24), 1744.

[5] J.-L. Lagrange, "On the figure of the columns" (in French), *Miscellanea Taurinensia*, vol. 5, pp. 123–166, 1770.

[6] J.-L. Lagrange, *On the figure of the columns(in French)*. In Oeuvres de Lagrange V. 2; Serret, M.J.A., Ed.; Gauthier-Villars: Paris, 1868.

[7] E. Kacapor, T.M. Atanackovic, and C. Dolicanin, "Optimal shape and first integrals for inverted compressed column," *Mathematics*, vol. 8, no. 3, p. 334, 2020, doi: 10.3390/math8030334.

[8] N. Olhoff and A.P. Seyranian, "Bifurcation and post-buckling analysis of bimodal optimum columns," *Int. J. Solids Struct.*, vol. 45, no. 14, pp. 3967–3995, 2008, doi: 10.1016/j.ijsolstr.2008.02.003.

[9] T.M. Atanackovic and A.P. Seyranian, "Application of pontryagin's principle to bimodal optimization problems," *Struct. Multidiscip. Optim.*, vol. 37, no. 1, pp. 1–12, 2008, doi: 10.1007/s00158-007-0211-6.

[10] M. Beck, "The buckling load of the cantilevered, tangentially compressed bar," *Z. Angew. Math. Phys.*, vol. 3, no. 3, pp. 225–228, 1952, doi: 10.1007/BF02008828.

[11] Y.M. Ghugal and R.P. Shimpi, "A review of refined shear deformation theories for isotropic and anisotropic laminated beams," *J. Reinf. Plast. Compos.*, vol. 20, no. 3, pp. 255–272, 2001, doi: 10.1177/073168401772678283.

[12] S. Timoshenko and J. Gere, *Theory of Elastic Stability*, 2nd ed. McGraw-Hill Book Co. Inc., 1961.

[13] I. Elishakoff, "Who developed the so-called timoshenko beam theory?" *Math. Mech. Solids.*, vol. 25, no. 1, pp. 97–116, 2020, doi: 10.1177/1081286519856931.

[14] W. Bickford, "A consistent higher order beam theory," in *Int. Proceeding of Dev. in Theoretical and Applied Mechanics (SECTAM)*, 1982, vol. 11, pp. 137–150.

[15] J.N. Reddy, "A simple higher-order theory for laminated composite plates," *J. Appl. Mech.*, vol. 51, no. 4, pp. 745–752, Dec 1984, doi: 10.1115/1.3167719.

[16] J.N. Reddy, *Theory and Analysis of Elastic Plates and Shells*. CRC Press, Nov 2006, doi: 10.1201/9780849384165.

[17] I. Elishakoff, Y. Li, and J.H. Starnes Jr., *Non-Classical Problems in the Theory of Elastic Stability*. Cambridge: Cambridge University Press, Jan. 2001, doi: 10.1017/cbo9780511529658.

[18] O.N. Kirillov, *Nonconservative Stability Problems of Modern Physics*. Berlin/Boston: De Gruyter, Jun. 2013, doi: 10.1515/9783110270433.

[19] Yuwaraj M. Ghugal and A.G. Dahake, "Flexure of cantilever thick beams using trigonometric shear deformation theory," *Int. J. Mech., Ind. Aerosp. Sci.*, 2014, doi: 10.5281/ZENODO.1336484.

[20] H.H. Leipholz, "Aspects of dynamic stability of structures," *J. Eng. Mech. Div.*, vol. 101, no. 2, pp. 109–124, Apr 1975, doi: 10.1061/jmcea3.0002000.

[21] C. Sundararajan, "On the flutter and divergence of a two-degree-of-freedom elastic system subjected to follower forces," *Z. Angew. Math. Mech.*, vol. 53, no. 11, pp. 801–802, 1973, doi: 10.1002/zamm.19730531111.

[22] Z. Kordas and M. Życzkowski, "On the loss of stability of a rod under a super-tangential force," *Arch. Mech. Stos.*, vol. 15, no. 1, pp. 7–31, 1963.

[23] C. Sundararajan, "Influence of an elastic end support on the vibration and stability of Beck's column," *Int. J. Mech. Sci.*, vol. 18, no. 5, pp. 239–241, May 1976, doi: 10.1016/0020-7403(76)90005-9.

[24] D. Bigoni and G. Noselli, "Experimental evidence of flutter and divergence instabilities induced by dry friction," *J. Mech. Phys. Solids*, vol. 59, no. 10, pp. 2208–2226, Oct 2011, doi: 10.1016/j.jmps.2011.05.007.

[25] A. Kounadis, "The existence of regions of divergence instability for nonconservative systems under follower forces," *Int. J. Solids Struct.*, vol. 19, no. 8, pp. 725–733, 1983, doi: 10.1016/0020-7683(83)90067-7.

[26] J. Gołaś and A. Niespodziana, "On influence the shear of deformation for Beck's column stability with local discontinuous," *Arch. Civ. Eng.*, vol. 54, no. 3, pp. 477–491, 2008.

[27] L. Tomski and S. Uzny, "The regions of flutter and divergence instability of a column subjected to beck's generalized load, taking into account the torsional flexibility of the loaded end of the column," *Mech. Res. Commun.*, vol. 38, no. 2, pp. 95–100, Mar 2011, doi: 10.1016/j.mech rescom.2011.01.013.

[28] W. Szemplińska-Stupnicka, *Application of parametric differential equations in mechanics and technology*. Warszawa: Pr. IPPT PAN, 1, Warszawska Drukarnia Naukowa, 1975, (in Polish).

[29] J. Gołaś and A. Niespodziana, "The dynamic stability of a stepped cantilever beam with attachments," *J. Vibroengineering*, vol. 15, no. 1, pp. 280–290, 2013.

[30] W. Sochacki, "Modelling and analysis of damped vibration in hydraulic cylinder," *Math. Comput. Model. Dyn. Syst.*, vol. 21, no. 1, pp. 23–37, Jan 2014, doi: 10.1080/13873954.2013.871564.

[31] W. Sochacki and M. Bold, "Vibration of crane radius change system with internal damping," *J. Appl. Math. Comput. Mech.*, vol. 12, no. 2, pp. 97–103, Jun 2013, doi: 10.17512/jamcm.2013.2.12.

[32] M. Bold and W. Sochacki, "Influence of complex damping on transverse and longitudinal vibrations of portal frame," *J. Vibroengineering*, vol. 21, no. 1, pp. 1–10, 2019.

[33] M. Bold and W. Sochacki, "Coupled vibration of cracked frame with damping," *Acta Phys. Pol. A*, vol. 138, no. 2, pp. 236–239, Aug 2020, doi: 10.12693/aphyspola.138. 236.

[34] J. Giergiel, *Mechanical vibrations of discrete systems*. Rzeszów: Oficyna wydawnicza Politechniki Rzeszowskiej, 2004, (in Polish).

[35] B. Żółtowski and S. Niziński, *Modeling of machine operation processes*. Bydgoszcz: Wydawnictwo Makar – B.Ż., 2002, (in Polish).

[36] Z. Osiński, *Damping of mechanical vibrations*. Warszawa: PWN, 1979, (in Polish).

[37] J. Giergiel, *Mechanical Vibration Damping, College Scripts No. 920*. Kraków: AGH, 1984, (in Polish).

[38] T. Soong and B. Spencer, "Supplemental energy dissipation: state-of-the-art and state-of-the-practice," *Eng. Struct.*, vol. 24, no. 3, pp. 243–259, Mar 2002, doi: 10.1016/s0141-0296(01)00092-x.

[39] Z. Osiński, *Vibration theory*. Warszawa: PWN, 1980, (in Polish).

[40] J.-W. Liang and B.F. Feeny, "Identifying Coulomb and viscous friction in forced dual-damped oscillators," *J. Vib. Acoust.*, vol. 126, no. 1, pp. 118–125, Jan 2004, doi: 10.1115/1.1640356.

[41] J. Walker, D. Halliday, and R. Resnick, *Fundamentals of physics. vol. 2*. Warszawa: PWN, 2014, (in Polish).

[42] M. Gürgöze, A. Doğruoğlu, and S. Zeren, "On the eigencharacteristics of a cantilevered visco-elastic beam carrying a tip mass and its representation by a spring-damper-mass system," *J. Sound Vib.*, vol. 301, no. 1-2, pp. 420–426, Mar 2007, doi: 10.1016/j.jsv.2006.10.002.

[43] J. Przybylski, *Vibrations and stability of prestressed two-member bar systems under non-conservative loads*, ser. Monographs no. 92. Częstochowa: Politechnika Częstochowska, 2002.

[44] M. Gürgöze and H. Erol, "Dynamic response of a viscously damped cantilever with a viscous end condition," *J. Sound Vib.*, vol. 298, no. 1-2, pp. 132–153, Nov 2006, doi: 10.1016/j.jsv.2006.04.042.

[45] S. Krenk, "Complex modes and frequencies in damped structural vibrations," *J. Sound Vib.*, vol. 270, no. 4-5, pp. 981–996, Mar 2004, doi: 10.1016/s0022-460x(03)00768-5.

[46] K. Jamroziak, M. Bocian, and M. Kulisiewicz, "Examples of applications of non-classical elastic-damping models in the ballistic impact process," *Modelowanie Inżynierskie*, vol. 40, pp. 95–102, 2010, (in Polish).

[47] K. Jamroziak, "Influence of dry friction on impact energy dissipation," *Wybrane Problemy Inżynierskie*, vol. 2, pp. 139–144, 2011, (in Polish).

[48] M.D. Rosa, M. Lippiello, M. Maurizi, and H. Martin, "Free vibration of elastically restrained cantilever tapered beams with concentrated viscous damping and mass," *Mech. Res. Commun.*, vol. 37, no. 2, pp. 261–264, Mar 2010, doi: 10.1016/j.mech rescom.2009.11.006.

[49] V. Jovanovic, "A fourier series solution for the transverse vibration response of a beam with a viscous boundary," *J. Sound Vib.*, vol. 330, no. 7, pp. 1504–1515, Mar 2011, doi: 10.1016/j.jsv.2010.10.007.

[50] H.A. Evensen and R.M. Evan-Iwanowski, "Effects of longitudinal inertia upon the parametric response of elastic columns," *J. Appl. Mech.*, vol. 33, no. 1, pp. 141–148, 1966, doi: 10.1115/1.3624971.

[51] I. Kovacic, R. Rand, and S.M. Sah, "Mathieu's equation and its generalizations: Overview of stability charts and their features," *Appl. Mech. Rev.*, vol. 70, no. 2, Feb 2018, doi: 10.1115/1.4039144.

[52] R.H. Rand, *Lecture Notes on Nonlinear Vibrations (Version 53)*. Ithaca, NY: Cornell University, 2017.

[53] J.D. Cole, *Perturbation Methods in Applied Mathematics*. Waltham: Blaisdell Pub. Co, 1968.

[54] A. Nayfeh, *Perturbation Methods*. New York: Wiley, 1973.

[55] P. Obara and W. Gilewski, "Dynamic stability of moderately thick beams and frames with the use of harmonic balance and perturbation methods," *Bull. Pol. Acad. Sci. Tech. Sci.*, vol. 64, no. 4, pp. 739–750, Dec 2016, doi: 10.1515/bpasts-2016-0083.

[56] M. Burzyńska–Szyszko, *Construction materials*. Warszawa: Politechnika Warszawska, 2011, (in Polish).